Available online at www.sciencedirect.com

SciVerse ScienceDirect

Ceramics International 39 (2013) 3715–3720

CERAMICS INTERNATIONAL

www.elsevier.com/locate/ceramint

Electrochemical synthesis and surface characterization of hexagonal Cu–ZnO nano-funnel tube films

Farid Jamali-Sheini[a,*], Ramin Yousefi[b]

[a]Department of Physics, Ahwaz Branch, Islamic Azad University, Ahwaz, Iran
[b]Department of Physics, Masjed-Soleiman Branch, Islamic Azad University (I.A.U), Masjed-Soleiman, Iran

Received 26 August 2012; received in revised form 16 October 2012; accepted 16 October 2012
Available online 23 October 2012

Abstract

An electrochemical deposition technique was used to synthesis hexagonal nano-funnel tube films on zinc foil, utilizing an electrolyte of $ZnCl_2+H_2O_2$ under ambient conditions. The structures, morphologies, chemical compositions, and optical properties of the synthesized films were characterized using X-ray diffractometry (XRD), scanning electron microscopy (SEM), transmission electron microscopy (TEM), UV–visible diffuse reflectance spectrometry (UV-vis-DRS), photoluminescence (PL) spectrometry, and energy-dispersive X-ray spectrometry (EDS) techniques. The XRD pattern showed a set of diffraction peaks that were indexed to the ZnO, $Zn(OH)_2$, and Cu phases. The SEM observations revealed a cauliflower-like morphology consisting of branches in the form of nano-funnel tubes. The TEM results demonstrated that the synthesized film was comprised of several branches. The EDS studies confirmed the presence of only Cu, Zn, and O atoms. The UV-vis-DRS spectrum showed the onset of the band gap absorption peak at ~375 nm. The PL studies evaluated various emission bands that originated from different defect mechanisms. In addition, the hexagonal nano-funnel tube film showed a good superhydrophobicity, with a water contact angle of ~153°.

Keywords: Electrochemical deposition; ZnO; Nano-funnel tube; Dendrite

1. Introduction

The chemical and physical properties of nanomaterials depend on their composition phase, structure, shape, size, and size distribution. Therefore, the architecture of a nanostructure with a controlled shape is important. In addition, to tailor and/or enhance the properties of synthesized nanostructures/films, many efforts have been made to composite and/or dope with other elements using different routes. Despite all these efforts, it is essential to try to synthesize novel shapes using a simple and low cost method.

Over the past few years, various kinds of nanostructures have been synthesized using a large number of techniques. Among these, ZnO nanostructures have received considerable attention because of their properties. These include a wide direct band gap energy (3.37 eV) and large excitation binding energy (60 meV) at room temperature, which suggest numerous possible practical applications. In addition, ZnO seems to have the richest family of nanostructures among all of the materials tested, including particles, rods, tubes, wires, nails, belts, marigolds/multipods, flowers, rings, helixes/springs, etc. [1–8].

Among the different methods for fabricating ZnO nanostructures (undoped/doped), the electrochemical deposition technique is an excellent one for synthesizing and controlling the shape and composition. This is done by tuning the reaction and reaction rate based on electrode potential and current density, respectively. Through such techniques, deposited films are strongly adherent to the substrate and are comprised of aggregated nanocrystallites. In addition, this technique is a simple and low cost technique that does not require a vacuum.

To date many methods have been used to fabricate various morphologies for Cu composited/doped ZnO nanostructures to modify their chemical and physical properties, including thermal evaporation [9], thermal

*Corresponding author. Tel.: +98 611 3348420x24; fax: +98 611 3329200.
E-mail addresses: faridjamali2003@yahoo.com, faridjamali@iauahvaz.ac.ir (F. Jamali-Sheini).

0272-8842/$ - see front matter © 2012 Elsevier Ltd and Techna Group S.r.l. All rights reserved.
http://dx.doi.org/10.1016/j.ceramint.2012.10.207

oxidation [10], electrodeposition [11,12], solvothermal [13], and so on. For instance, Zhang et al. reported Cu-doped ZnO nanoneedles and nanonails using a thermal evaporation system [9]. They found that, there is a strong correlation between the morphology and the optical properties. They also observed the ferromagnetism property in the produced nanomaterials. In our previous work, Cu–ZnO nanoneedle arrays were synthesized using a vacuum evaporation system and thermal oxidation process. The results showed an enhancement in the field emission properties [10]. We also used the electrodeposition method to synthesis a composite of Cu/ZnO [11]. Because of the presence of Cu atoms in the ZnO structures, as compared with the undoped ZnO structures, a different optical property was observed. Similarly, enhanced field emission properties were obtained. In addition, based on our experience obtained through the electrochemical deposition technique, different parameters such as the electrolyte concentrations and composition, pH, temperature, stirring, and applied voltage could affect the morphology of the produced materials [11]. Thus, in order to find the effects of these parameters on the morphology, systematic studies have been carried out. It was found that at a particular voltage, electrolyte concentration (without stirring the solution), temperature, and time deposition, hexagonal Cu–ZnO nano-funnel tube films could be synthesized. Another research group has made an effort to show the ability of the electrochemical deposition method to produce Cu-doped ZnO nanowires with the optical properties tuned by the doping [12]. Recently, some results have shown that Cu–ZnO nanostructures are good candidates for many applications. For example, Zhao et al. synthesized Cu-doped ZnO nanofibers using electrospinning technology for H_2S sensing [13]. Finally, Cu–ZnO nanostructures may have different applications and using the electrochemical deposition method is an effective and promising approach to synthesize metal ion-doped ZnO nanostructures.

Accordingly, in the present work, we report the synthesis of hexagonal Cu–ZnO nano-funnel tube films on a zinc foil using an electrochemical deposition method. The structural, chemical, and optical properties of the obtained films were characterized by different techniques such as X-ray diffractometry, electron microscopies, and energy-dispersive X-ray, UV–visible, and photoluminescence spectrometers. The water contact angle was also measured.

2. Experimental section

The synthesis of Cu–ZnO films was performed in a conventional three-electrode electrochemical cell. An aqueous solution containing a mixture of $ZnCl_2$, $CuCl_2$, and H_2O_2 (analytical grade) with concentrations of $\sim 16\times10^{-3}$ M, 1×10^{-3} M, and 40×10^{-3} M, respectively, was used as an electrolyte. All of the deposition experiments were carried out at 82 °C, in which a polycrystalline Zn foil (99.99% pure, Alfa Aesar), platinum sheet, and saturated calomel electrode (SCE, $E_0=0.244$ V vs. NHE) served as the working, counter, and reference electrodes, respectively. Prior to the deposition, the Zn foil (substrate) and platinum electrode were ultrasonically cleaned in acetone and methanol successively for 10 min. A computer controlled electrochemical analyzer (Model-1100 A Series, CH Instrument, USA) was used to maintain the cathodic polarization condition at -2.2 V with respect to the SCE. The electrolyte was kept fixed without stirring during the synthesis and, after a certain deposition time (30 min), the working electrode was removed from the electrolyte, washed in a gentle flow of water, and dried in air. At least four specimens were synthesized under identical experimental conditions and characterized by various analytical techniques in order to check the reproducibility and repeatability of the results.

The synthesized films were characterized using an X-ray diffractometer (XRD) (D8, Advance, Bruker AXS) with CuKα (λ: 1.5406 Å) as the radiation. The scanning electron microscope (SEM) observation was carried out (JEOL, JSM-6360 A) using an operating voltage of 20 kV and an emission current of ~60 μA. The elemental composition was obtained using an energy-dispersive X-ray spectrometer (EDS) attached to the SEM instrument with the operating voltage of 20 kV. The collection time was 80 s and four spots were analyzed (~25 μm^2 each). For the transmission electron microscope (TEM) analysis, (Philips, EM-CM-12) the specimens were prepared by scraping the Cu–ZnO film from the substrates. The scraped material was dispersed and sonicated in acetone. A small quantity of this solution was dropped on the TEM grid. The optical properties were investigated using the UV–visible (UV–vis) and photoluminescence (PL) spectra recorded at room temperature. The UV–vis diffuse reflectance spectra (DRS) were recorded using a UV–visible spectrophotometer (JASCO, UV-670) over a wavelength range of 200–800 nm. The PL was measured with a photoluminescence spectrometer (Perkin Elmer, LS-55) using a xenon lamp as the source with an excitation wavelength of ~305 nm. The water contact angle (WCA) measurement was performed using a homemade measurement system at ambient temperature. Small water droplets (5 mL) were dropped on the surface of the specimen and the WCA was recorded using a digital camera. The WCAs were obtained at four different points on each specimen by measuring the angle between the surface of the specimen and the water droplet boundary on the surface.

3. Results and discussion

A typical XRD pattern of the synthesized film is shown in Fig. 1. The XRD pattern reveals a set of diffraction peaks, which are indexed to the wurtzite hexagonal phase of ZnO and $Zn(OH)_2$ by comparing the observed *d*-values with the standard JCPDS data [ZnO card no. 80-0075 and $Zn(OH)_2$ card no. 76-1778]. In order to obtain the optimum conditions for the growth, $Zn(OH)_2$ could not

be completely converted into ZnO. In addition, a peak corresponding to Cu was indexed [card no. 85-1326]. The appearance of the diffraction peaks corresponding to Zn was caused by the fact that Zn foil was used as a substrate. The sharp and strong diffraction peaks indicate that the synthesized film was well-crystalline. Further, no characteristic diffraction peaks from other phases or impurities were found.

Fig. 2 shows the typical SEM images of the synthesized film at different magnifications. A cauliflower-like morphology consisting of branch shapes deposited on the substrate can be observed from Fig. 2a and b. A careful observation (Fig. 2b) indicates well-defined dendritic structures growing radially from a single nucleation center, resulting in a few branch assemblies. The lengths of these branches range from 500 nm to several microns. As can be clearly seen from the high magnification images (Fig. 2c and d), a typical morphology was identified, consisting of a structure with one open end, well-defined crystallographic facets, and hollow hexagonal cross-sections, which is called a hexagonal Cu–ZnO nano-funnel tube. It can also be seen that there is a possibility for the growth of a nano-funnel tube from the inside and central part of another hexagonal Cu–ZnO nano-funnel tube. An average nano-funnel tube is 300 nm–1 μm in length and 300–600 nm in diameter.

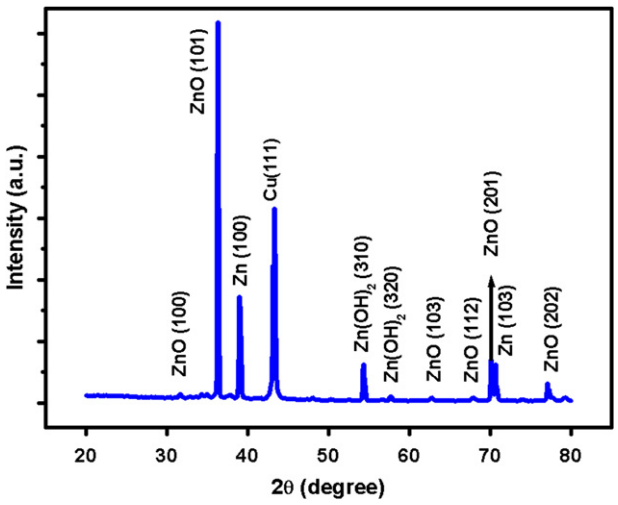

Fig. 1. XRD pattern of the hexagonal Cu–ZnO nano-funnel tube film grown on zinc substrate.

The compositional analysis and purity of the synthesized films were obtained using the EDS technique. The typical EDS spectrum of the synthesized film (Fig. 3) shows the presence of Cu, Zn, and O, with atomic percentages of 15.47%, 54.42%, and 30.11%, respectively.

In order to evaluate the structural features of the synthesized Cu–ZnO film, TEM investigations were carried out. A typical TEM image is shown in Fig. 4a, indicating a cauliflower-like morphology, consisting of a branch shape with a nano-scale structure (30–70 nm) without symmetrical growth. This result is in good agreement with the SEM observations. Because of the thickness of the branch structures, no nano-funnel tube is resolved. The selected area electron diffraction (SAED) pattern was obtained from circular area of the branch structures on the TEM grid. The SAED pattern reveals spotty rings, which were identified by Cu particles and ZnO nano-branches.

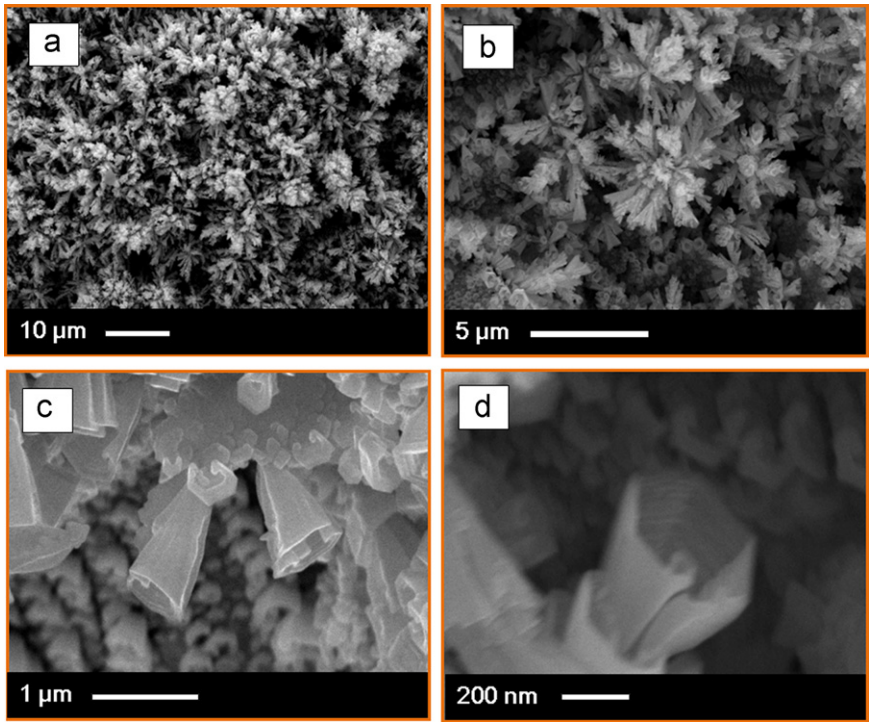

Fig. 2. (a, b) low and (c, d) high magnified SEM images of the hexagonal Cu–ZnO nano-funnel tube film.

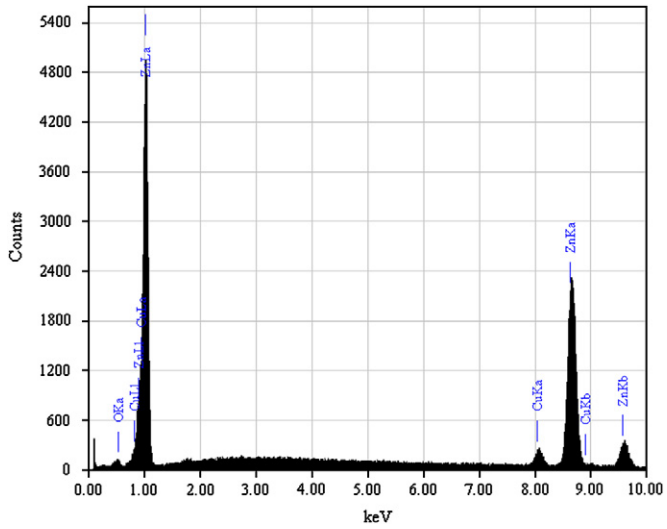

Fig. 3. EDS spectrum of the hexagonal Cu–ZnO nano-funnel tube film.

It is expected that the ring-like pattern can be indexed to ZnO (002), (103) and Cu (111), (200), (220) diffractions.

The UV–visible diffused reflectance (DRS) and photoluminescence (PL) spectrometers were used to examine the optical properties of the synthesized films. Fig. 5a depicts a typical DRS plot of the hexagonal Cu–ZnO nano-funnel tube film grown on the zinc substrate. The apparent onset of the absorption band for the film is ~375 nm. The maximum absorption band edge is located at ~335 nm. According to the equation $Eg = 1240/\lambda$, the calculated Eg from the onset of reflectance is 3.30 eV. This value is lower than the bulk value of the ZnO band gap (3.37 eV). In addition, the obtained result is in accordance with our previous report [10]. The PL of the hexagonal Cu–ZnO nano-funnel tube film is shown in Fig. 5b. As can be seen, there are several peaks at 375, 410, 424, 447, 470, and 519 nm. The ultraviolet emission band located at 375 nm is attributed to the near-band edge (NBE) free exciton transition from the localized level below the conduction band to the valance band [14]. The violet, blue, and green emission bands are observed at 410, 424, 447, 470, and 520 nm, respectively. They originate from different deep-level emissions (DLEs). These DLEs are mainly related to point defects such as the oxygen vacancies and zinc interstitials. Cheng et al. [15] attributed the appearance of blue emission bands to the oxygen vacancy. Vanheusden et al. [16], on the other hand, attributed the green transition to the singly ionized oxygen vacancy in the ZnO, and the emission results from the recombination of the photogenerated hole with the singly ionized charge also point to such a defect. The blue–green emission can originate from oxygen vacancies, Zn interstitials, extrinsic defects, or impurities [17,18]. Thus, it is believed that during the deposition, copper ions can replace either substitutional and/or interstitial zinc ions in the ZnO lattice, creating point defects (Cu_{Zn}, Cu_i) and the structural deformation. It is expected that, because of the presence of

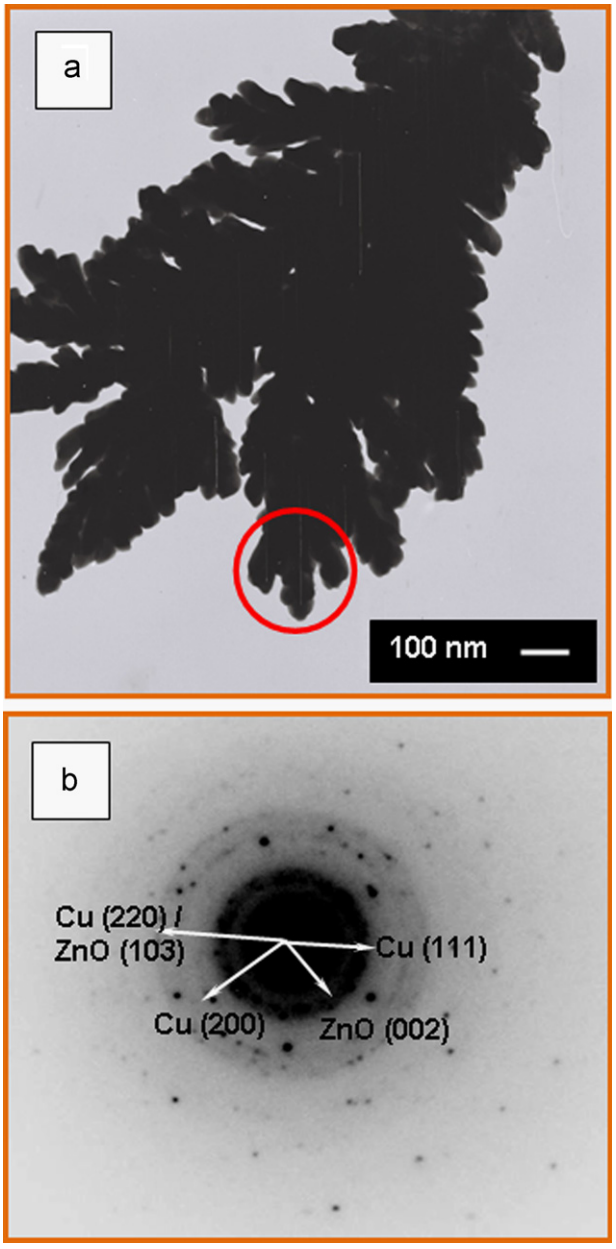

Fig. 4. (a) TEM image of nano-scale branch structures of the Cu–ZnO film and (b) the SAED pattern of red marked area.

oxygen vacancies and point defects, there is a possibility of using the synthesized film as a gas sensor.

Controlling and modifying the surface wettability are important in many practical applications [19]. The surface morphology and surface energy are two crucial factors to control the surface wettability. Thus, by changing the roughness of the surface and/or mixing with other materials, the wetting characteristics are expected to be modified. In general, the surface wettability is determined by its WCA and divided into two categories, hydrophilic (WCA < 90°) and hydrophobic (WCA > 90°). Fig. 6 shows the WCA image of the hexagonal Cu–ZnO nano-funnel tube film. It is observed that the WCA of the synthesized film is ~153°. This is consistent with the fact that the superhydrophobicity of the

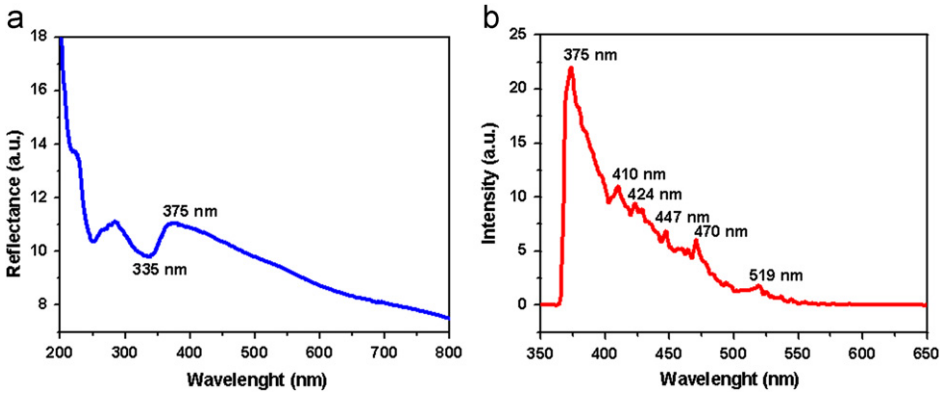

Fig. 5. (a) UV–visible DRS and (b) PL spectra of the hexagonal Cu–ZnO nano-funnel tube film.

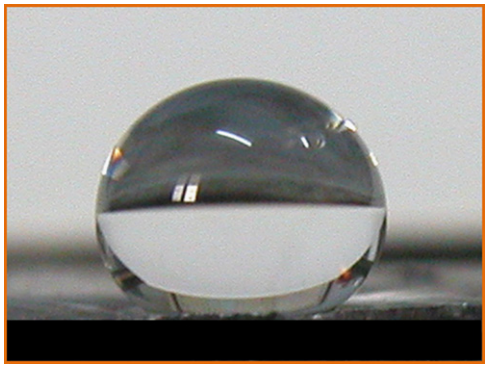

Fig. 6. WCA image of the hexagonal Cu–ZnO nano-funnel tube film grown on zinc substrate.

surfaces is caused by the air trapped between the water and rough surface. In addition, the branch structures with a tube shape would produce more cavities to trap air, which suspend the water droplets on the hexagonal Cu–ZnO nano-funnel tube film and generate the surface superhydrophobicity [20].

4. Conclusions

In summary, Cu–ZnO nano-funnel films were successfully synthesized using an electrochemical deposition technique under ambient conditions. XRD and SAED analyses revealed the presence of ZnO and Cu phases. In addition, a $Zn(OH)_2$ peak was observed in the XRD pattern. The SEM and TEM results both showed that the synthesized film consisted of hexagonal Cu–ZnO nano-funnel tubes with several branches. From the UV–vis absorption and PL spectra found, there was a decrease in the band gap energy with respect to the bulk value of the ZnO band gap. The hexagonal Cu–ZnO nano-funnel tube film showed an excellent superhydrophobicity, which suggests its importance for many practical applications. In addition, because of the hexagonal tube shape, there was a large effective surface area, which could be used for photocatalyst applications. This method could be employed to synthesize and control the shapes of other metal ion-doped ZnO nanostructures.

Acknowledgments

This work was financially supported by the Islamic Azad University, Ahwaz Branch, Ahwaz, Iran. F. Jamali-Sheini is grateful to Prof. P. B. Vidyasagar (Head of Department), Prof. D. S. Joag, and Prof. M. A. More from the Department of Physics, University of Pune, India, for their instrumentation support. R. Yousefi gratefully acknowledges the Islamic Azad University, Masjed-Soleiman Branch for their financial support of this research work.

References

[1] Z. Hu, D.J. Escamilla Ramírez, B.E. Heredia Cervera, G. Skam, P.C. Searson, Synthesis of ZnO nanoparticles in 2-propanol by reaction with water, Journal of Physical Chemistry B 109 (2005) 11209–11214.
[2] H. Yu, Z. Zhang, M. Han, X. Hao, F. Zhu, A general low-temperature route for large-scale fabrication of highly oriented ZnO nanorod/nanotube arrays, Journal of the American Chemical Society 127 (2005) 2378–2379.
[3] F. Jamali Sheini, I.S. Mulla, D.S. Joag, M.A. More, Influence of process variables on growth of ZnO nanowires by cathodic electrodeposition on zinc substrate, Thin Solid Films 517 (2009) 6605–6611.
[4] A. Qurashi, J.H. Kim, Y.-B. Hahn, Direct fabrication of ZnO nanorods array on-chip system in solution and their electrical properties, Electrochemistry Communications 18 (2012) 88–91.
[5] A. Qurashi, J.H. Kim, Y.-B. Hahn, Density-controlled selective growth of well-aligned ZnO nanorod arrays by a hybrid approach, Superlattices and Microstructures 48 (2010) 162–169.
[6] R. Yousefi, M.R. Muhamad, A.K. Zak, The effect of source temperature on morphological and optical properties of ZnO nanowires grown using a modified thermal evaporation set-up, Current Applied Physics 11 (2011) 767–770.
[7] X.Y. Kong, Y. Ding, R.S. Yang, Z.L. Wang, Single-crystal nanorings formed by epitaxial self-coiling of polar nanobelts, Science 303 (2004) 1348–1351.
[8] X.Y. Kong, Z.L. Wang, Spontaneous polarization-induced nanohelixes, nanosprings, and nanorings of piezoelectric nanobelts, Nano Letters 3 (2003) 1625–1631.
[9] Z. Zhang, J.B. Yi, J. Ding, L.M. Wong, H.L. Seng, S.J. Wang, J.G. Tao, G.P. Li, G.Z. Xing, T.C. Sum, C.H.A. Huan, T. Wu, Cu-Doped ZnO nanoneedles and nanonails: morphological evolution

and physical properties, Journal of Physical Chemistry C 112 (26) (2008) 9579–9585.
[10] F. Jamali-Sheini, K.R. Patil, D.S. Joag, M.A. More, Synthesis of Cu–ZnO and C–ZnO nanoneedle arrays on zinc foil by low temperature oxidation route: effect of buffer layers on growth, optical and field emission properties, Applied Surface Science 257 (2011) 8366–8372.
[11] F. Jamali Sheini, J. Singh, O.N. Srivasatva, D.S. Joag, M.A. More, Electrochemical synthesis of Cu/ZnO nanocomposite films and their efficient field emission behavior, Applied Surface Science 256 (2010) 2110–2114.
[12] O. Lupana, T. Pauportéa, B. Vianac, P. Aschehougc, Electrodeposition of Cu-doped ZnO nanowire arrays and heterojunction formation with p-GaN for color tunable light emitting diode applications, Electrochimica Acta 56 (2011) 10543–10549.
[13] M. Zhao, X. Wang, L. Ning, J. Jia, X. Li, L. Cao, Electrospun Cu-doped ZnO nanofibers for H_2S sensing, Sensors and Actuators B 156 (2011) 588–592.
[14] S. Cho, J. Ma, Y. Kim, Y. Sun, G.K.L. Wong, J.B. Ketterson, Photoluminescence and ultraviolet lasing of polycrystalline ZnO thin films prepared by the oxidation of the metallic Zn, Applied Physics Letters 75 (1999) 2761–2763.
[15] W. Cheng, P. Wu, X. Zou, T. Xiao, Study on synthesis and blue emission mechanism of ZnO tetrapod like nanostructures, Journal of Applied Physics 100 (2006) 054311–054313.
[16] K. Vanheusden, W.L. Warren, C.H. Seager, D.R. Tallant, J.A. Voigt, B.E. Gnade, Mechanisms behind green photoluminescence in ZnO phosphor powders, Journal of Applied Physics 79 (1996) 7983–7990.
[17] Y.G. Wang, S.P. Lau, H.W. Lee, S.F. Yu, B.K. Tay, X.H. Zhang, H.H. Hng, Photoluminescence study of ZnO films prepared by thermal oxidation of Zn metallic films in air, Journal of Applied Physics 94 (2003) 354–358.
[18] B. Lin, Z. Fu, Y. Jia, Green luminescent center in undoped zinc oxide films deposited on silicon substrates, Applied Physics Letters 79 (2001) 943–945.
[19] I.P. Parkin, G.R. Palgrave, Self-cleaning coatings, Journal of Materials Chemistry 15 (2005) 1689–1695.
[20] Y. Hu, S. Liu, S. Huang, W. Pan, Superhydrophobicity and surface enhanced Raman scattering activity of dendritic silver layers, Thin Solid Films 519 (2010) 1314–1318.